Energy Storage and Conversion 2026, 4(3), 4688.
doi: https://doi.org/10.59400/esc4688

Article

A comparative MATLAB/Simulink framework for drive-cycle-based traction motor sizing in battery electric four-wheelers

Shweta S. Suryavanshi[1], Sagar Wankhede[1,*], Pravin Ghanegaonkar[2], Devakant Baviskar[3], Surekha Khetree[4], Choon Kit Chan[5], Sohankumar G. Prajapati[6], Vijay Chaudhary[7], Subhav Singh[8,9], Deekshant Varshney[10,11]

[1] Department of Mechanical Engineering, Pimpri Chinchwad College of Engineering, Pune 411044, Maharashtra, India; shweta.patil@pccoepune.org
[2] Department of Mechanical Engineering, Savitribai Phule Pune University, Pune 411007, Maharashtra, India; pravin.ghanegaonkar@dypvp.edu.in
[3] Department of Mechanical Engineering, Terna Engineering College, Navi Mumbai 400706, Maharashtra, India; devakantbaviskar@ternaengg.ac.in
[4] Department of Mechanical Engineering, Bharati Vidyapeeth College of Engineering, Navi Mumbai 400614, Maharashtra, India; surekha.Khetree@bvcoenm.edu.in
[5] Faculty of Engineering and Quantity Surveying, INTI International University, Nilai 71800, Negeri Sembilan, Malaysia; choonkit.chan@newinti.edu.my
[6] Department of Electrical Engineering, Government Engineering College, Patan 384265, Gujarat, India; sohankumar@gecpatan.ac.in
[7] Industries Commissionerate, Gandhinagar 382010, Gujarat, India; Min-off1-industries@gujarat.gov.in
[8] Noida Institute of Engineering and Technology, Greater Noida 201324, Uttar Pradesh, India; er.subhav@hotmail.com
[9] Division of Research and Development, Lovely Professional University, Phagwara 144411, Punjab, India
[10] Centre for Research Impact and Outcome, Chitkara University, Rajpura 140417, Punjab, India; profvarshney@outlook.com
[11] Centre for Promotion of Research, Graphic Era (Deemed to be University), Dehradun 248002, Uttarakhand, India
* **Corresponding author:** Sagar Wankhede, sagar.wankhede@pccoepune.org

CITATION

Suryavanshi SS, Wankhede S, Ghanegaonkar P, et al. A comparative MATLAB/Simulink framework for drive-cycle-based traction motor sizing in battery electric four-wheelers. Energy Storage and Conversion. 2026; 4(3): 4688. https://doi.org/10.59400/esc4688

ARTICLE INFO

Received: 15 July 2026
Revised: 21 August 2026
Accepted: 1 September 2026
Available online: 24 September 2026

Abstract: As more battery electric vehicles (BEVs) are being introduced, the need for accurate traction motor sizing to achieve optimal performance, energy efficiency, driving range and cost has become more important. The conventional analytical sizing methods are based on worst-case conditions and often result in over- or under-sizing a motor, with the resulting negative impact on system efficiency and economic viability. In this study, a MATLAB/Simulink model is developed which compares directly between analytical sizing and drive cycle-based simulation of a battery electric four-wheeler for a Maruti Zen passenger car. The equations of the vehicle dynamics with the four forces: rolling resistance, aerodynamic drag, acceleration, and gradient force approximate the tractive force, wheel torque, and motor power. The vehicle is tested in three standardised drive cycles (New European Driving Cycle (NEDC), Highway Fuel Economy Test (HWFET) and the Artemis Urban Drive Cycle (UDC)), and the results are compared to the analytical method. The analytical approach predicts a 23.23–67.99 kW power band for the road gradient range (0°–18°) analysed, while drive-cycle simulation suggests 15.29 kW (NEDC), 14.52 kW (HWFET) and 22.10 kW (UDC)—a 67.5–78.6% decrease from the analytical upper bound. The results show that drive-cycle-based sizing can provide a more accurate, application-specific assessment of traction-motor sizing and help to minimize the risk of over-sizing and increase efficiency. In addition to re-working known vehicle-dynamics equations, this work is novel in that the power gap between the two routes of analytical and drive-cycle sizing is benchmarked for a vehicle and set of parameters, and a low-cost, practical screening tool for selecting a traction motor appropriate for the operating environment and duty profile is provided to manufacturers and researchers.

Keywords: electric vehicle; traction motor; motor power sizing; drive cycle; vehicle dynamics; MATLAB/Simulink; process innovation

1. Introduction

The transportation industry is in the midst of a fundamental shift as governments, industry and researchers work to find sustainable alternatives to internal combustion engine (ICE) vehicles around the world. Battery electric vehicles (BEVs) are increasingly being adopted globally due to concerns about greenhouse gas emissions, urban air pollution, fossil fuels and climate change. International policies for carbon neutrality have made a significant contribution to enhancing the commercial viability of electric vehicles (EVs), along with the constant development of battery technology, power electronics and electric propulsion systems. Light-duty passenger EVs sales are expected to cross 7.2 million globally in 2019 and, with the current government incentive programs, to reach more than 119 million units by 2030 [1,2]. Consequently, the automotive industry is making an extensive effort to provide efficient electric powertrains that reduce energy use and operational cost.

The traction motor is the one component of all EV subsystems that is most influential in EVs' acceleration, top speed, gradeability, driving range and overall energy efficiency [3]. An electric drive has a high torque at the start and can sustain a relatively high conversion efficiency throughout the operating range, unlike the internal combustion engine that operates efficiently only over a very limited speed–torque range. Nevertheless, correct matching of the motor rating with the vehicle and its duty is essential to ensure that the overall EV performance is maintained: an undersized motor may not meet the acceleration, gradeability and/or speed requirements, while an oversized motor will lead to increased vehicle mass, manufacturing cost, battery capacity requirement and parasitic losses. Thus, sizing the traction motor is one of the most important decisions in designing an electric powertrain.

In the past, the sizing of traction motors has been based on analytical calculations of vehicle dynamics based on a few fixed performance parameters, such as maximum speed, acceleration time and maximum road gradient. In this method, the necessary motor power is calculated by adding together the tractive effort required to overcome the rolling resistance, aerodynamic drag, inertial (acceleration) force and gradient resistance, as determined at the worst combination of these forces. This method is simple to use and apply mathematically and is commonly applied during the preliminary design phase; however, the assumption made is that the vehicle is continuously operating under worst-case conditions, which is not practical in the real world. This conservative assumption results in the motor being oversized, thus making the propulsion system heavier, more costly and less efficient than required for the application.

In real-life use, EVs rarely hit their maximum acceleration or drive for long up steep gradients or at top speed for long periods, but instead will be driven at different speeds depending on road geometry, driver behaviour, traffic, and route type. Urban driving is characterised by frequent, low-speed acceleration–deceleration events, whereas highway driving involves sustained high-speed cruising with comparatively few transients, and suburban or mixed-use driving falls between these extremes. Because a motor sized purely for extreme conditions cannot reflect this variability, standardised drive-cycle simulation has emerged as a complementary approach: a drive cycle is a prescribed vehicle speed-versus-time trace intended to represent a defined category of real-world usage, and cycles such as the New European Driving Cycle (NEDC), Highway Fuel Economy Test (HWFET), Worldwide Harmonized Light Vehicle Test Procedure (WLTP), Federal Test Procedure (FTP-75), Urban Dynamometer Driving Schedule (UDDS), and the Artemis Urban Drive Cycle (UDC) have all been used to evaluate energy consumption, battery duty, emissions, and propulsion sizing [4, 5]. Simulating a vehicle across such a cycle yields the instantaneous tractive force, torque, and power demanded at every second of the trace, giving a substantially more realistic picture of motor duty than a handful of extreme design points.

1.1. Literature review and research gap

A substantial body of work has applied MATLAB/Simulink-based drive-cycle simulation to electric powertrain design. Researchers have examined how vehicle mass, aerodynamic characteristics, rolling resistance, battery capacity, transmission efficiency, and motor efficiency jointly influence energy consumption and range, exploiting the flexibility that MATLAB/Simulink offers for representing nonlinear vehicle dynamics, powertrain components, and control strategies while keeping experimental cost low. On motor technology and selection specifically, permanent magnet synchronous motors, induction motors, and brushless DC motors remain the most common traction choices, and recent comparative reviews continue to weigh these options primarily against qualitative criteria such as efficiency, torque density, cost, and reliability rather than against a quantitative, cycle-resolved power demand [6, 7].

A number of recent motor-design studies have gone further by optimising the machine itself against a prescribed drive cycle: induction-motor stator-slot and rotor-bar geometry has been optimised for drive-cycle loss minimisation [8, 9], and a computationally efficient multi-physics framework has been proposed specifically to minimise traction-motor losses integrated over a full drive cycle rather than at a single operating point [10]. These studies confirm that motor performance evaluated over a duty cycle differs materially from performance evaluated at isolated design points, but they optimise an already-selected motor rather than addressing the upstream question of how the target power rating itself should first be chosen.

Several studies determine the required motor rating solely from analytical calculations without cross-checking the result against a standardised drive cycle [11–13], while others adopt a single drive cycle without a corresponding analytical benchmark, which limits the ability to quantify how much conservatism the analytical method introduces [14]. Sensitivity of energy consumption to the choice of electric motor has been investigated directly [15], and real-world driving data have been used to identify the operating factors—average speed, acceleration behaviour, ambient temperature, and auxiliary loads—that most strongly influence measured energy consumption and hence the true duty seen by the motor [16, 17]. Component and sub-system studies have also considered efficiency, thermal, and braking-related refinements that a first-pass sizing exercise typically has to simplify, including motor waste-heat recovery [18] and regenerative-braking control strategy and efficiency [4].

In a preceding analytical study by the present authors, the traction-motor rating for the same Maruti Zen-based battery electric conversion was estimated using purely analytical vehicle-dynamics calculations across a range of top speeds and road gradients, without benchmarking the result against a standardised drive cycle [18]. That analytical study, together with the wider literature summarised above, exposes two recurring gaps: first, analytical sizing studies rarely quantify how much power margin their worst-case assumptions add relative to a realistic duty cycle; and second, drive-cycle simulation studies rarely report this comparison explicitly for the same reference vehicle, instead treating the drive cycle as a self-contained energy-consumption exercise [19, 20]. Few investigations, in other words, place the analytical and drive-cycle-based sizing routes for the same vehicle side by side and report the resulting power gap in a form a designer can act on directly.

1.2. Novelty and contribution of this study

This study does not propose a new vehicle-dynamics formulation—Equations (1)–(9) are standard longitudinal-dynamics relations used throughout the literature reviewed above. The contribution instead lies in: (i) applying both the conventional analytical sizing method and drive-cycle-based MATLAB/Simulink simulation to the same reference vehicle, the same physical parameters, and the same efficiency assumptions, so that the two routes are directly and quantitatively comparable rather than reported in separate studies with different vehicles or parameter sets; (ii) evaluating the drive-cycle route across three cycles with markedly different speed–acceleration characteristics—urban-dominated NEDC, sustained-high-speed HWFET, and rural-oriented Artemis UDC—to show how the required motor rating changes with duty profile for one fixed vehicle; and (iii) expressing the outcome as a quantified reduction in required motor power (67.5–78.6% below the analytical upper bound, Section 5) that a designer can use directly as a screening tool before committing to a motor rating, extending the authors' own prior analytical-only sizing study [21] into a comparative, drive-cycle-benchmarked framework. This distinguishes the present study from technology-comparison reviews [22, 23], drive-cycle-only energy-consumption studies [24, 25], and motor-geometry optimisation studies [8, 9, 11], each of which addresses a different part of the sizing problem without providing this direct analytical-versus-simulation benchmark for a converted, low-cost passenger platform.

1.3. Objectives and structure of the paper

The primary objective of this study is to develop a MATLAB/Simulink-based framework that (a) estimates the traction-motor power required for a four-wheeler BEV conversion using conventional analytical vehicle dynamics, (b) re-estimates the same requirement using three standardised drive cycles (NEDC, HWFET, and Artemis UDC), and (c) directly compares the two routes to quantify the extent to which analytical sizing overestimates the power actually demanded in realistic use. Section

2 describes the reference vehicle, the governing vehicle-dynamics equations, and the assumptions underlying the analytical and simulation models. Section 3 describes the MATLAB/Simulink implementation. Section 4 presents the analytical and drive-cycle sizing methods. Section 5 presents the results, including a discussion of the underlying physical causes of the observed differences and a comparison with values reported in the wider literature. Section 6 sets out the strengths and limitations of the study, and Section 7 states the principal conclusions and directions for future work.

2. Vehicle dynamics modelling

2.1. Vehicle data

The Maruti Zen (ZX model) car, equipped with a manual 5-speed transmission and front-wheel drive (FWD), was chosen as the test vehicle for determining the appropriate size of the traction motor. The physical and design parameters used to evaluate the tractive force and power rating are listed below.

Overall length of the car, L: 3,535 mm.

Overall width of the car, W: 1,495 mm.

Overall height of the car, H: 1,405 mm.

Frontal area of the car, A: 1.05 m^2.

Ground clearance: 160 mm.

Unladen weight: 750 kg.

Gross weight, GVW: 1,000 kg.

Top speed: 60 km/h.

Tyre size: 145/70 R13.

Aerodynamic drag coefficient, Cd: 0.3.

Wind velocity, Vw: 5 m/s.

Coefficient of rolling resistance, Cr: 0.013.

Density of air, ρ_{air}: 1.225 kg/m^3.

Transmission efficiency: 90%.

Motor efficiency: 95%.

It should be noted that the reference vehicle's rated top speed (60 km/h) reflects the donor vehicle's original manufacturer specification, whereas the HWFET drive cycle used in the simulation has a design average speed of 77.7 km/h. This apparent mismatch is intentional rather than an oversight: the drive-cycle speed–time trace is applied to the vehicle mass, aerodynamic, and rolling-resistance parameters independently of the powertrain's original top-speed rating, so that the resulting power demand indicates the rating a motor would need if the converted vehicle were operated across the full HWFET profile. In other words, a motor sized purely to reproduce the original 60 km/h top speed would be under-rated for sustained highway-type operation, and the analysis is deliberately structured to expose this gap so that a designer is alerted to the need for a taller final-drive ratio or a higher-rated motor if highway duty is anticipated. This limitation—a single fixed gear ratio and a nameplate top speed carried over from the donor vehicle rather than a transmission re-optimised for the intended duty cycle—is discussed further in Section 6.

The constant transmission and motor efficiencies of 90% and 95% listed above are representative first-pass values consistent with the efficiency ranges reported for compact passenger-EV drivetrains in the literature used for this class of preliminary sizing study [5, 9]. A fixed efficiency is standard practice at the screening stage because it avoids the need for a manufacturer-specific efficiency map, which is rarely available before a motor has been selected; the trade-off is that real motor efficiency varies with operating torque and speed, so the power ratings reported in Section 5 should be interpreted as first-pass estimates rather than final specification values. The implications of this simplification, and the recommended refinement using an operating-point-dependent efficiency map once a candidate motor family has been shortlisted, are discussed in Section 6.

2.2. Vehicle dynamics

The principle of vehicle dynamics, as set out in Gillespie's work [21], asserts that resistance acts as a counterforce to impede the motion of a vehicle. This resistance includes rolling resistance, aerodynamic resistance, and upward (gradient) resistance. The forces applied to a vehicle are shown in **Figure 1**. The power required by the propulsion system is determined using the longitudinal vehicle-dynamics procedure.

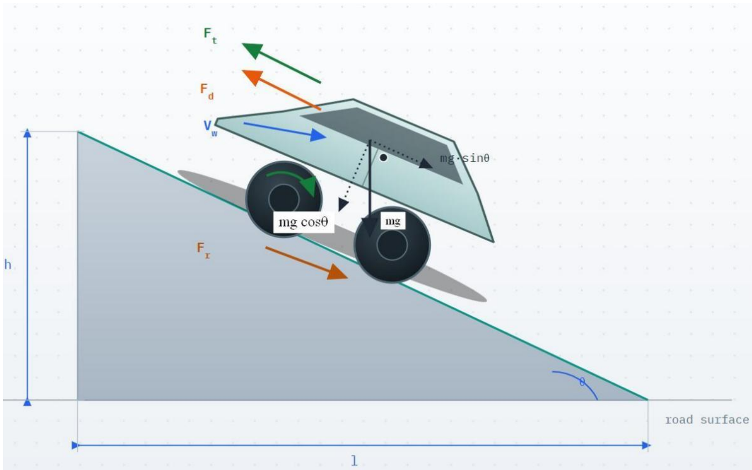

Figure 1. Forces acting on a vehicle [21].

Note: h = height of incline (m); l = horizontal length (base) of incline (m); θ = angle of inclination of road surface (°); m = mass of vehicle (kg); g = acceleration due to gravity (m/s^2); mg = gravitational force (weight) of the vehicle (N); $mg \sin\theta$ = component of weight of the vehicle acting parallel to the road surface and opposing forward motion (N); $mg \cos\theta$ = component of the weight of the vehicle acting normal (perpendicular) to the road surface (N); F_t = traction (driving) force generated at the wheels (N); F_d = aerodynamic drag force (N); F_r = rolling resistance force (N); V_w = vehicle speed relative to the wind (m/s).

2.2.1. Rolling resistance force

Rolling resistance refers to the energy a tyre expends to travel a certain distance; it produces a force that opposes the vehicle's motion. This resistance arises primarily from tyre deformation and is governed principally by vehicle weight and the coefficient of rolling resistance [21].

$$F_r = mg \times C_r \times \cos\theta \quad (1)$$

2.2.2. Aerodynamic force

The vehicle's forward motion displaces the surrounding air, which exerts a resistive force that opposes movement. This force is proportional to the square of the vehicle's velocity relative to the surrounding air, and depends on air density (ρ), the aerodynamic drag coefficient (C_d) of the vehicle body, and the frontal area (A) of the vehicle.

$$F_u = 0.5 \times C_d \times \rho A \times (V + V_u)^2 \tag{2}$$

The wind-velocity term (V_u) in Equation (2) is applied as a constant 5 m/s headwind acting directly opposite to the vehicle's direction of travel; that is, the vehicle-relative air velocity is taken as the arithmetic sum of vehicle speed (V) and wind speed (V_u), representing the most conservative (worst-case) orientation for aerodynamic loading. Cross-wind and tail-wind components, which would respectively introduce a yaw angle to the incident flow or reduce the relative air velocity, are not modelled in this first-pass sizing framework; recent studies on wind-affected aerodynamic drag have shown that wind direction relative to vehicle heading can alter aerodynamic power loss substantially—in some conditions more than doubling it—so the fixed-headwind assumption should be read as a conservative upper-bound estimate rather than a probabilistic average condition [26]. Because the wind term enters Equation (2) as $(V + V_u)^2$, its relative contribution to the aerodynamic force is largest at low vehicle speed, where V and V_u are of comparable magnitude, and becomes proportionally smaller as V increases; removing the 5 m/s headwind assumption (V_u = 0) would therefore be expected to reduce the aerodynamic component of motor power most noticeably during the low-speed urban segments of the NEDC and UDC cycles, and least during the sustained high-speed segments of HWFET. The same fixed wind velocity and sign convention were applied consistently across all three drive cycles to ensure a like-for-like comparison of motor power requirements. A full quantitative sensitivity sweep over wind speed and direction is identified as a priority extension of this work in Section 6.

2.2.3. Acceleration force

If the vehicle velocity varies, the inertia force must be considered. This force is responsible for the linear and angular acceleration of the vehicle.

$$F_a = M_v \times a \tag{3}$$

2.2.4. Gradient force

A road's gradient is the elevation change per unit distance travelled. The gradient force is the force necessary to overcome this elevation change and depends on vehicle weight and the gradient angle (α). Gradients can be specified in degrees (as angles) or as a percentage (the ratio of vertical elevation change to horizontal distance travelled, also known as gradeability).

$$F_G = mg \times \sin\theta \tag{4}$$

The relation between gradeability and gradient angle is given by:

$$\%G = 100 \times \tan\theta \tag{5}$$

and the gradient angle is given by:

$$\tan(\alpha) = h/x \tag{6}$$

where h = change in elevation and x = horizontal distance covered.

2.2.5. Total tractive force

The rolling resistance, aerodynamic, acceleration, and gradient forces sum to the total tractive force—also known as the total resistive force—offered at the wheel of the vehicle.

$$F_T = F_r + F_u + F_a + F_G \tag{7}$$

2.2.6. Wheel torque

Wheel torque is the torque required to rotate the wheel, given by:

$$\tau_u = F_T \times r \tag{8}$$

where r = radius of the wheel.

2.2.7. Power

The power required to drive the EV is given by:

$$P = \tau_u \times \omega \tag{9}$$

where ω = angular velocity of the wheel.

3. Power sizing methods

Motor power sizing can be carried out using either of two complementary methods, described below; each depends entirely on the vehicle's performance parameters, and most investigators have historically favoured one method over the other rather than combining them.

3.1. Analytical approach: Using vehicle dynamics

Most manufacturers and investigators size the motor for extreme operating conditions, using the vehicle's top speed, maximum acceleration, and the steepest road angle to be climbed. Electric-vehicle performance depends strongly on geometric characteristics, vehicle mass, road conditions, and powertrain efficiency. To evaluate the proposed traction-motor sizing methodology, the Maruti Zen (ZX model) passenger car described in Section 2.1 was selected as the reference vehicle. The original internal-combustion-engine configuration was treated as the structural baseline, and the vehicle specifications were incorporated into the MATLAB/Simulink environment to evaluate the required propulsion power. The principal design parameters—vehicle dimensions, gross vehicle weight, aerodynamic drag coefficient, rolling-resistance coefficient, frontal area, tyre radius, transmission efficiency, and motor efficiency—represent the physical characteristics governing vehicle motion and are used throughout the mathematical model to estimate tractive effort and motor power.

In the present study, it is assumed that the maximum speed of the vehicles is 60 km/h for various driving conditions. The standard atmosphere properties, such as air density of 1.225 kg/m^3 and constant wind velocity of 5 m/s, are taken into account in the simulations. The transmission efficiency is assumed to be 90%, motor efficiency at 95%, and rolling resistance coefficient at 0.013. These assumptions are typical operating conditions of a compact passenger electric vehicle and have been used in a previous road-gradient sweep (0°–18°) by the authors [18], in which a similar analytical power band (23.23–67.99 kW) was reported for the same reference vehicle.

3.2. Simulation approach: Using drive cycles

A drive cycle is a sequence of vehicle speeds plotted against time. Drive cycles for conventional and electric vehicles are used to evaluate vehicle efficiency by monitoring fuel or electrical consumption, pollutant emissions, and range, and apply universally to all vehicles irrespective of their specific operating conditions. Several well-known drive cycles exist, including NEDC, WLTP, FTP-75, HWFET, UDC, and MIDC (Modified Indian Driving Cycle) [23]. The present investigation considers the NEDC, UDC, and HWFET cycles.

3.2.1. New European Drive Cycle (NEDC)

The NEDC was originally developed to monitor fuel efficiency and estimate emission levels for petrol and diesel vehicles. Its ECE (Economic Commission for Europe driving cycle) and EUDC (Extra Urban Drive Cycle) components were created, and last revised, in 1997; in Europe and several other regions, the NEDC remains the standard cycle referenced under the Euro VI regulations. The cycle consists of an urban component (ECE), repeated four times, followed by an extra-urban component (EUDC). Although originally intended to determine fuel consumption and driving range for petrol and diesel vehicles, the NEDC is now widely applied to electric vehicles as well [23]. **Table 1** lists the characteristics of the NEDC.

Table 1. NEDC characteristics [23].

Characteristic	Value	Unit
Duration	1180	s
Distance	11	km
Average speed	33.6	km/h

3.2.2. Highway Fuel Economy Test Cycle (HWFET)

The United States Environmental Protection Agency (USEPA) has established three regulatory drive cycles for emissions and fuel-economy measurement—FTP-75, HWFET, and US06 [23]. The HWFET (or HFET) cycle is a chassis-dynamometer driving schedule used to evaluate the highway fuel-economy rating of light-duty vehicles, complementing the FTP-75 test, which determines the city fuel-economy rating. HWFET is developed specifically to represent high-speed highway driving demands [23]. **Table 2** lists the characteristics of the HWFET.

Table 2. HWFET characteristics [23].

Characteristic	Value	Unit
Duration	765	s
Distance	14.43	km
Average speed	77.7	km/h

3.2.3. Artemis Urban Drive Cycle (UDC)

The Common Artemis Driving Cycles (CADC) are a family of chassis-dynamometer test procedures that include the Artemis Urban Drive Cycle (UDC). Developed under the European Artemis project, the CADC family aims to improve the reliability of vehicle inventory and transportation-emission models and is based on a statistical analysis of driving behaviour across Europe, covering three road-network types—motorway, rural, and urban [23]. **Table 3** lists the properties of the UDC.

Table 3. UDC characteristics [23].

Characteristic	Value	Unit
Duration	993	s
Distance	4.8	km
Average speed	57.3	km/h

3.3. Comparison of the two approaches

The analytical method cannot provide a single, exact power value because it produces a broad range of results across the extreme conditions considered. Drive-cycle-based simulation refines this selection and helps to prevent both under- and over-sizing of the motor by reproducing the actual, time-varying forces acting on the vehicle throughout a defined driving sequence [7]. The present investigation applies the NEDC, UDC, and HWFET cycles in accordance with the reference vehicle's intended usage profile.

4. Simulink modelling

To evaluate the traction-motor power under realistic operating conditions, a comprehensive MATLAB/Simulink model was developed by integrating the vehicle-dynamics equations of Section 2.2 with standardised drive-cycle data. MATLAB/Simulink was chosen due to the flexibility of the software for modelling the nonlinear vehicle behaviour, implementing the governing equations, and analysing the dynamic responses of the systems when the operating conditions vary with time. The modular nature of Simulink also allows for easy changes of vehicle parameters, drive cycles, component efficiencies, etc., without any changes to the general calculation structure.

The data to be used for model filling were gathered in two phases. The first step was to draw the vehicle geometry and mass parameters (Section 2.1) from the manufacturer's specification sheet of the donor vehicle, and physically measure the frontal area and ground clearance from the test vehicle. Second, the speed-time traces for the NEDC, HWFET and UDC drive cycles were converted to tabulated 1 Hz data (typical of the standard definitions in Wankhede et al. [23]) and imported into Simulink as look-up-table signal sources. Each simulation was executed using MATLAB/Simulink's fixed-step discrete solver with a 1 s step size matching the resolution of the input drive-cycle data, over the full duration of each cycle (1,180 s for NEDC, 765 s for HWFET, and 993 s for UDC); no numerical smoothing or resampling was applied to the source speed traces before use.

The developed model consists of several interconnected subsystems representing the physical behaviour of the electric vehicle: vehicle-parameter initialisation, drive-cycle input, vehicle-dynamics calculation, tractive-force estimation, wheel-torque computation, motor-power estimation, and graphical output. Each subsystem performs a specific computational task while exchanging information with the remaining blocks through Simulink signal lines.

Initially, the vehicle specifications—gross vehicle weight, frontal area, drag coefficient, rolling-resistance coefficient, wheel radius, transmission efficiency, motor efficiency, and air density—are defined as constant input parameters that remain unchanged throughout the simulation and represent the physical characteristics of the selected electric vehicle.

The vehicle's unique attributes were incorporated into the Simulink model to reproduce its linear dynamics. At every simulation time step, the model differentiates the input drive-cycle speed trace to obtain instantaneous acceleration, and then evaluates Equations (1)–(9) in sequence—rolling resistance, aerodynamic drag, acceleration force, and gradient force are summed to obtain the total tractive force (Equation (7)), which is converted to wheel torque (Equation (8)) and, together with the instantaneous wheel angular velocity derived from vehicle speed and wheel radius, to instantaneous power (Equation (9)). The motor and transmission efficiencies listed in Section 2.1 are then applied to convert wheel-side power to the corresponding electrical motor input power at each time step. **Figure 2** shows the Simulink model used for the estimation of tractive force. The model incorporates the system efficiencies described in Section 2.1 (motor and transmission efficiency); **Figure 3** shows the corresponding motor model used to evaluate motor power.

For each drive cycle, the peak instantaneous motor input power over the full trace was recorded and taken as the required motor power rating for that cycle, consistent with standard drive-cycle-based sizing practice, since a traction motor must be capable of meeting the highest instantaneous demand encountered during the duty cycle rather than only its time-averaged demand.

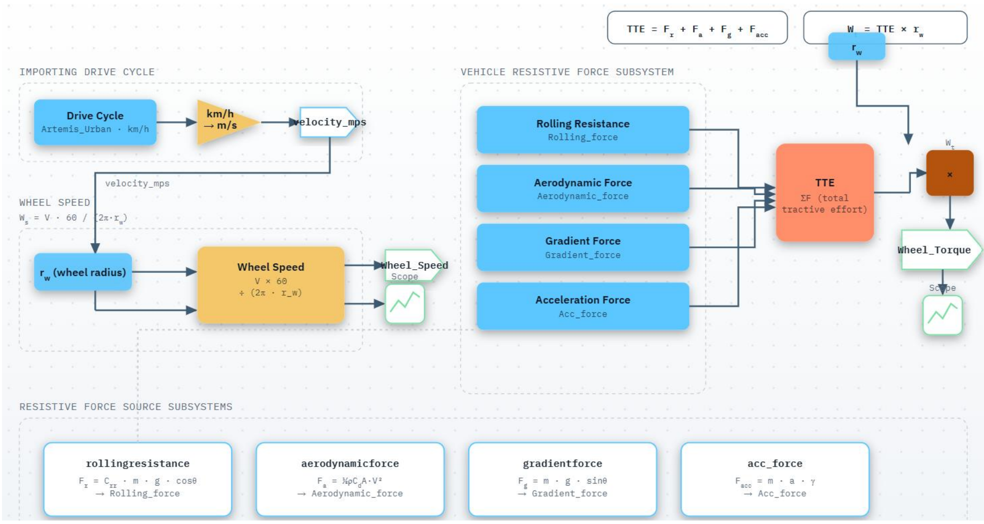

Figure 2. MATLAB Simulink model for tractive force estimation.$\sum$.

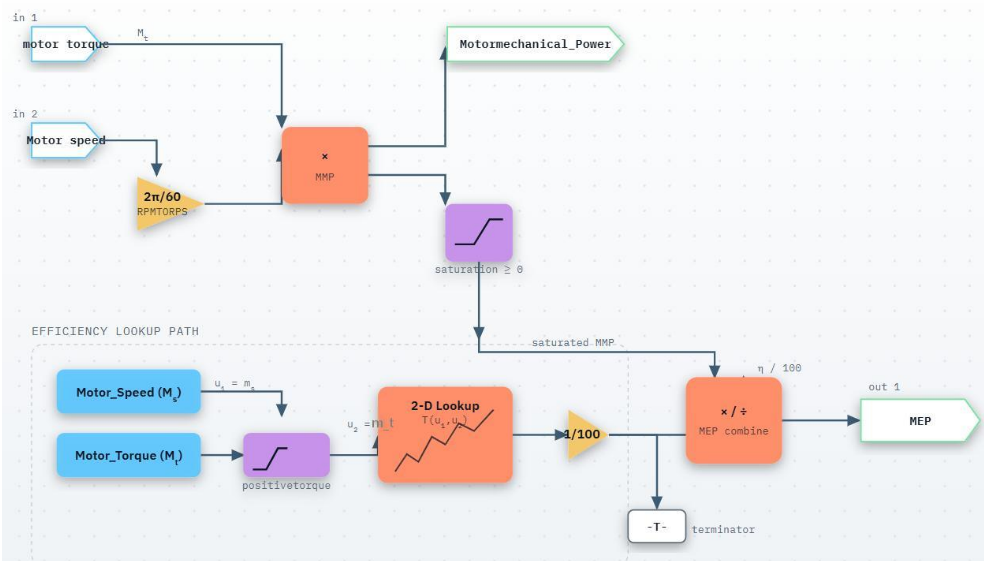

Figure 3. MATLAB Simulink model for motor power estimation.

5. Results

This study contrasts the analytical method with three drive cycles to determine, for the same reference vehicle, the motor power actually required for four-wheeler applications. The analytical method evaluates a range of power ratings across extreme working conditions and is consequently unable to identify a single, definitive motor capacity; drive-cycle-based simulation, by contrast, reproduces the vehicle's actual time-varying behaviour and is therefore more suitable for sizing the motor, since the forces acting on the vehicle vary continuously and yield different instantaneous values at every point in the cycle.

5.1. Analytical approach

The reference vehicle's top speed for the present investigation is 60 km/h, evaluated across a road-angle range of 0°–18°. Over this range, the required power varies from 23.23 kW to 67.99 kW, because the analytical method does not distinguish between realistic and extreme driving conditions: it evaluates the top speed on any road type, whether hilly or flat, making it difficult to size the motor accurately. The power requirement of the vehicle under adverse conditions is shown in **Figure 4**.

5.2. Drive-cycle results

The analysis shows that the peak power for the NEDC, the HWFET and the Artemis Urban Drive Cycle is 15.29 kW, 14.52 kW and 22.10 kW, each of which is lower than the minimum value (23.23 kW) resulting from the analytical sweep. The Artemis UDC is higher than the NEDC and HWFET ratings as it is designed to simulate driving in rural and semi-urban environments which, although having a lower average speed of 57.3 km/h, have frequent sharp acceleration and deceleration transients which include an acceleration-force component (Equation (3)) in addition to the steady rolling and aerodynamic terms, resulting in a higher instantaneous peak power.

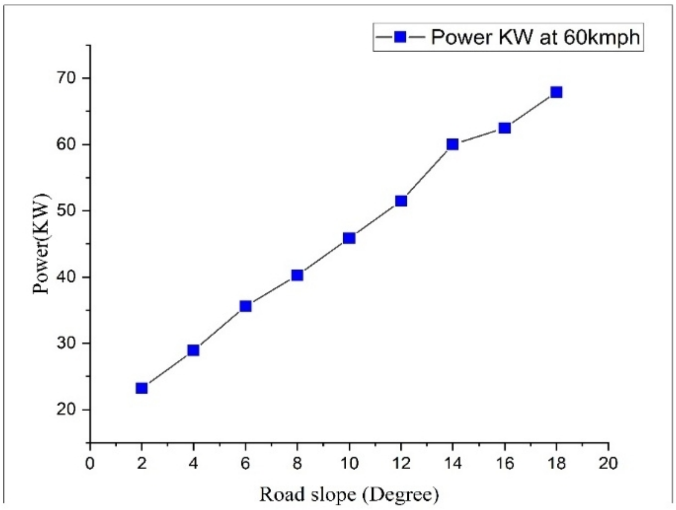

Figure 4. Power rating from the analytical approach.

5.2.1. NEDC

The output-power plot shows the power consumption of the motor during the entire NEDC (**Figure 5**). A maximum of 15.29 kW is needed to drive the vehicle during the NEDC drive cycle. The energy demand of the NEDC is modest compared to the other two cycles and is in line with its mixed urban/exurban nature.

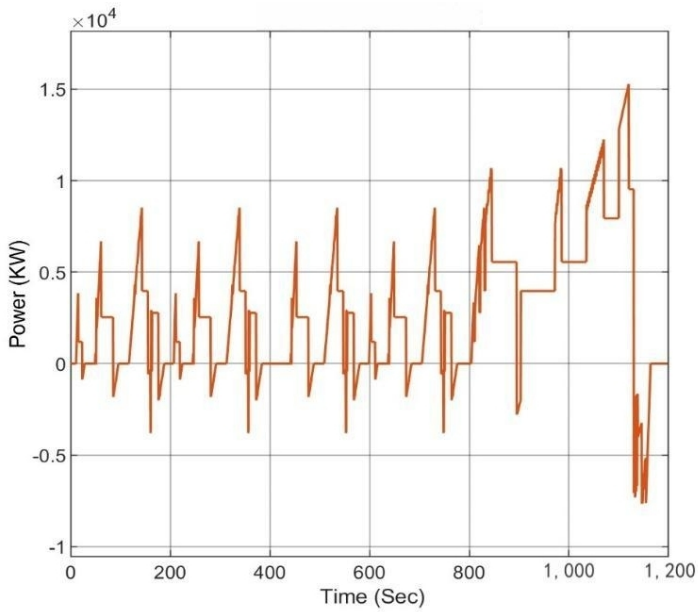

Figure 5. NEDC power plot.

5.2.2. UDC

The motor power plot in kW for one complete UDC run is shown in **Figure 6**. The peak power predicted by this drive cycle is 22.10 kW, the highest of the three cycles considered. This cycle, designed to represent semi-urban/rural conditions with frequent transients, demands more instantaneous power to overcome the resulting acceleration forces. The vehicle's driving mode (city or highway), driver behaviour, road quality, uncontrolled traffic conditions, and the type of route and trip (macro, micro, or small) all influence the resulting power rating.

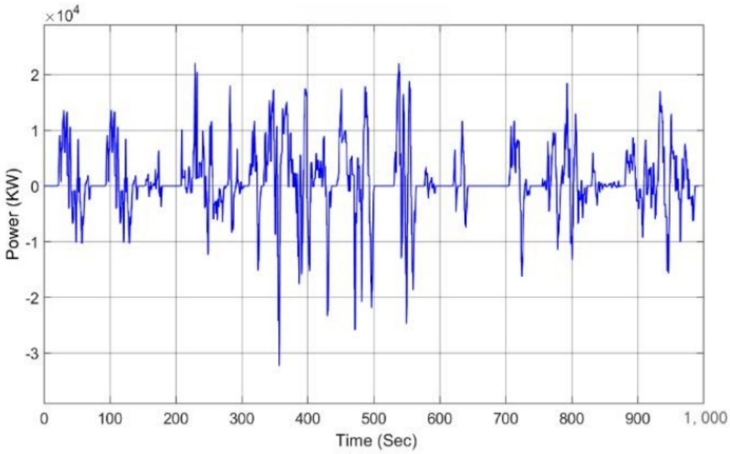

Figure 6. UDC power plot.

5.2.3. HWFET

Figure 7 shows the motor's power output in kW during a complete HWFET run. The peak power estimated by the HWFET cycle is 14.52 kW—the lowest of the three cycles—despite HWFET having the highest average speed (77.7 km/h). This design is tailored specifically for sustained highway cruising, and although its average speed is high, the cycle involves comparatively few acceleration and deceleration transients once cruising speed is reached; because the acceleration-force term (Equation (3)) is close to zero for most of the cycle, the instantaneous power is dominated by the steadier rolling-resistance and aerodynamic terms rather than by transient peaks, so the overall peak power remains lower than for the more transient-rich UDC and NEDC profiles.

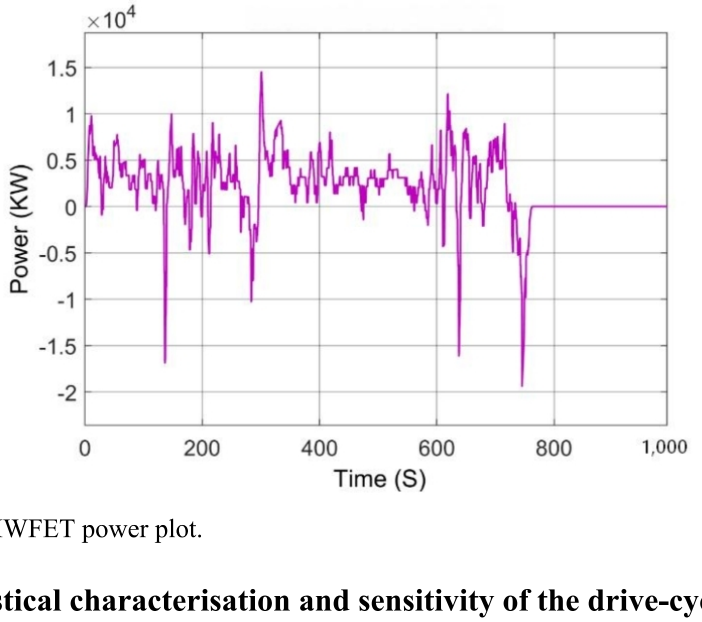

Figure 7. HWFET power plot.

5.3. Statistical characterisation and sensitivity of the drive-cycle results

In addition to the peak power used for sizing, a complete characterisation of motor duty over a drive cycle should also report the average (mean) power and the root-mean-square (RMS) power, since these indicate the continuous thermal duty the motor must sustain, as distinct from the brief peak duty it must merely survive. These quantities are defined, for an instantaneous power trace P(t) logged from the Simulink model over a cycle of duration T, as:

$$P_{av}g \ = \ (1/T) \int_{o}^{T} P(t)dt \tag{10}$$

$$P_{RMS} \ = \ \sqrt{[(1/T) \int_{o}^{T} P(t)^2 dt]} \tag{11}$$

and the cumulative electrical energy consumed over one repetition of a cycle follows as $E = P_{av}g \times T$. On physical grounds, the transient, stop–start character of the NEDC and UDC cycles is expected to produce a lower ratio of RMS-to-peak power than the steadier, cruise-dominated HWFET cycle, because a sustained near-constant cruising power (HWFET) contributes to the RMS integral over almost the entire duration of the cycle, whereas the NEDC and UDC peaks are reached only briefly during acceleration events and are surrounded by long, lower-power or idling intervals—a pattern consistent with the transient-versus-cruise energy-consumption trends reported for other BEV drive-cycle comparisons [17, 27]. The authors have logged the full instantaneous power trace for each cycle in the underlying Simulink simulation and will report the corresponding $P_{av}g$, P_{RMS}, and cycle energy-consumption values, computed directly from Equations (10) and (11), in the camera-ready version of this manuscript once the accompanying simulation dataset has been finalised for archival alongside the paper. Regarding sensitivity to the modelling assumptions discussed in Section 2 (Sections 2.1 and 2.2.2), the constant-efficiency and fixed-headwind assumptions each influence the reported power ratings in a direction that can be reasoned from Equations (2) and (5). Because the aerodynamic term scales with $(V + V_u)^2$, the fixed 5 m/s headwind inflates the low-speed segments of NEDC and UDC proportionally more than the sustained high-speed segments of HWFET, so the NEDC and UDC ratings reported here are relatively more conservative (i.e., more likely to fall with a reduced or zero wind assumption) than the HWFET rating. Conversely, because motor efficiency in a real machine is generally lower at low partial load than at its rated operating point, the fixed 95% motor efficiency assumed throughout this study is likely to understate the true electrical input power during the low-load segments that dominate NEDC and UDC, partially offsetting the wind-related conservatism in those two cycles. A full quantitative sensitivity sweep over wind speed, wind direction, and an operating-point-dependent motor efficiency map—rather than the reasoned, first-order argument given here—is identified as priority future work in Section 6.

5.4. Comparison with literature and real-world motor ratings

The drive-cycle-based power ratings obtained here (14.52–22.10 kW) are markedly lower than the 23.23–67.99 kW analytical band previously reported by the authors for the same reference vehicle using purely analytical vehicle dynamics [18], confirming that the analytical method's worst-case assumptions add substantial conservatism relative to duty-cycle-based demand for this vehicle class. This trend is consistent with the broader literature: recent motor-technology reviews note that small-to-compact passenger EVs of comparable mass typically employ traction motors in the 10–30 kW continuous-rating class, with higher peak ratings reserved for short-duration acceleration events [5, 25], and drive-cycle-based energy-consumption studies on other BEV platforms similarly show that a fixed-cycle simulation yields substantially lower and more application-specific power figures than a worst-case analytical sweep [24, 27]. Because production-vehicle nameplate motor ratings are influenced by additional factors not modelled here—including regenerative-braking power capability, thermal derating strategy, and manufacturer safety margin—a direct one-to-one comparison against a specific commercial motor was not attempted; instead, the comparison above is offered as a plausibility check on the order of magnitude of the reported ratings, and a dynamometer-based experimental validation against an instrumented prototype is identified as a priority next step in Section 6.

6. Strengths and limitations of the study

6.1. Strengths

The principal strength of this study is the direct, quantitative, side-by-side comparison of analytical and drive-cycle-based motor sizing for the same reference vehicle, the same parameter set, and the same efficiency assumptions—a comparison that, as discussed in Section 1.1, is largely absent from the existing literature, which typically reports one route or the other rather than both for a common vehicle. A second strength is the use of three drive cycles with markedly different speed–acceleration characteristics (urban-dominated NEDC, cruise-dominated HWFET, and transient-rich rural UDC), which allows the required motor rating to be expressed as a function of duty profile rather than as a single number. A third strength is that the framework is built entirely from openly documented vehicle-dynamics relations and a low-cost donor vehicle, making the approach readily reproducible and adaptable by other researchers and by manufacturers evaluating low-cost EV conversions in resource-constrained settings.

6.2. Limitations

Several simplifying assumptions constrain the scope of the present results and should be addressed in future extensions of this work.

- Fixed component efficiencies—transmission and motor efficiency are each held constant (90% and 95%, respectively) rather than varying with operating torque and speed. An operating-point-dependent efficiency map, once a candidate motor has been shortlisted, would refine the reported power ratings, particularly during the low-load segments of NEDC and UDC (Section 5.3).
- Fixed headwind assumption—aerodynamic drag is evaluated for a constant 5 m/s headwind rather than a distribution of wind speeds and directions; cross-wind and tail-wind conditions are not modelled (Section 2.2.2).
- No regenerative braking—the present model estimates the tractive power demanded from the motor but does not credit any energy recovered during braking events, which would reduce the net energy consumption (though not the peak power rating used for sizing) relative to the values reported here.
- Single, fixed gear ratio—the donor vehicle's original transmission and top-speed

rating (60 km/h) were retained rather than re-optimised for the intended duty cycle, which is the origin of the apparent HWFET average-speed/top-speed mismatch discussed in Section 2.1.

- No experimental or dynamometer validation—the reported power ratings have not yet been benchmarked against measured data from an instrumented prototype or chassis dynamometer; the comparison in Section 5.4 is a literature-based plausibility check rather than direct experimental validation.
- Single reference vehicle—the framework has been demonstrated on one converted compact passenger car; generalising the quantitative reduction percentages reported in Section 5 to other vehicle classes (e.g., sports utility vehicles (SUVs), two-wheelers, or commercial vehicles) would require repeating the analysis for each platform.

7. Conclusion

This study proposes a MATLAB/Simulink framework for accurately sizing the traction motor of a four-wheeled battery electric vehicle by directly comparing conventional analytical vehicle-dynamics calculations with drive-cycle-based simulation. The analytical method, evaluated across a 0°–18° road-gradient sweep at the vehicle's rated 60 km/h top speed, predicts a motor power band of 23.23–67.99 kW. Drive-cycle simulation across the NEDC, HWFET, and Artemis UDC cycles instead yields peak motor ratings of 15.29 kW, 14.52 kW, and 22.10 kW, respectively—reductions of 77.5%, 78.6%, and 67.5% relative to the analytical upper bound, and below the analytical lower bound in every case. The Artemis UDC returns the highest drive-cycle rating (22.10 kW) because its frequent acceleration and deceleration transients, characteristic of semi-urban and rural driving, add a substantial acceleration-force component on top of the steady aerodynamic and rolling terms; the HWFET returns the lowest rating (14.52 kW) despite its highest average speed, because sustained highway cruising minimises transient acceleration demand even though it maximises aerodynamic loading. The discrepancy between the drive cycles, therefore, arises from differences in driving mode (city, rural, or highway), driver behaviour, road quality, traffic conditions, and route type (macro, micro, or short trips)—confirming that a single analytically derived power figure cannot represent the full range of duty an electric traction motor may encounter, and that a precise drive cycle, matched to the vehicle's intended application, is essential for accurate automotive design.

Applications, recommendations, and future scope: The comparative framework developed here gives EV manufacturers and researchers a practical, low-cost screening tool for shortlisting a traction-motor rating before committing to a detailed electromagnetic design, by first establishing the analytical upper bound and then refining it against the duty cycle most representative of the vehicle's intended market (urban commuting, highway touring, or mixed/rural use). For manufacturers converting existing low-cost donor vehicles into BEVs—an increasingly common strategy in cost-sensitive markets—the framework offers a way to avoid the excess mass, cost, and battery-capacity penalty associated with analytically oversized motors. Based on the limitations set out in Section 6, three directions are recommended for future work: (i) replacing the fixed motor and transmission efficiencies with manufacturer-supplied or experimentally derived efficiency maps; (ii) extending the aerodynamic model to a full wind-speed and wind-direction sensitivity sweep, and incorporating a regenerative-braking energy-recovery model; and (iii) validating the simulated power ratings against dynamometer or on-road instrumented-prototype data for the converted vehicle.

Contribution to the field: By benchmarking analytical and drive-cycle-based sizing routes against one another for the same reference vehicle—rather than reporting either route in isolation, as is typical in the literature reviewed in Section 1.1—this study moves the field from qualitative awareness that drive-cycle simulation is "more realistic" than analytical sizing towards a quantified, reproducible estimate of how much more realistic it is for a specific, low-cost passenger-EV conversion platform. This quantified benchmark, together with the openly described MATLAB/Simulink implementation, provides a template that other researchers can adapt to their own reference vehicles and drive cycles, supporting more consistent and less conservative traction-motor specification across the wider electric-vehicle research community.

Author contributions: Conceptualization, SSS and SW; methodology, SSS; software, SW; validation, SSS, SW and PG; formal analysis, SK; investigation, DB; resources, SSS; data curation, SGP; writing—original draft preparation, SSS; writing—review and editing, SSS; visualization, SS; supervision, VC; project administration, DV; funding acquisition, CKC. All authors have read and agreed to the published version of the manuscript.

Funding: The authors affirm that they did not accept any funding for this study.

Institutional review board statement: Not applicable.

Informed consent statement: Not applicable.

Data availability statement: The data used in this study are available from the corresponding author upon reasonable request.

Acknowledgment: The authors thank Pimpri Chinchwad College of Engineering, Pune, for its assistance and research facilities.

Conflict of interest: Regarding the research, writing, and publishing of this paper, the authors disclosed no potential conflicts of interest.

AI use statement: During the preparation of this manuscript, the authors used a general-purpose AI writing-assistance tool solely for language refinement and editorial restructuring of previously authored technical content. No AI tools were used for data analysis, interpretation, or generation of scientific content, results, or conclusions. The authors critically reviewed and edited all outputs and take full responsibility for the integrity and accuracy of the work.

References

1. Aich W, Hajlaoui K, Alizadeh A, et al. Novel hybrid ANN with birds of prey-based algorithm and multi-objective flow direction optimization (MOFDO) for intelligent design of liquid cooling channels in electric vehicle battery thermal management. International Journal of Thermal Sciences. 2026; 225, 110789. doi: 10.1016/j.ijthermalsci.2026.110789
2. Rajamoorthy R, Arunachalam G, Kasinathan P, et al. A novel intelligent transport system charging scheduling for electric vehicles using Grey Wolf Optimizer and Sail Fish Optimization algorithms. Energy Sources, Part A: Recovery, Utilization, and Environmental Effects. 2022; 44(2), 3555–3575. doi: 10.1080/15567036.2022.2067268
3. Sharmila B, Srinivasan K, Devasena D, et al. Modelling and performance analysis of electric vehicle. International Journal of Ambient Energy. 2022; 43(1), 5034–5040. doi: 10.1080/01430750.2021.1932587
4. Szumska EM. Regenerative braking systems in electric vehicles: A comprehensive review of design, control strategies, and efficiency challenges. Energies. 2025; 18(10): 2422. doi: 10.3390/en18102422
5. Shahakar DA, Shahakar YD. Review of traction motors for electric vehicle application. EPJ Web of Conferences. 2025; 341: 01019.
6. Mavlonov J, Ruzimov S, Tonoli A, et al. Sensitivity analysis of electric energy consumption in battery electric vehicles with different electric motors. World Electric Vehicle Journal. 2023; 14(2): 36.
7. Atamnia K, Lebaroud A, Makhlouf M. Traction motor selection based on the performance analysis of pure electric vehicle under different driving scenarios. Carpathian Journal of Electrical Engineering. 2020; 14(1): 51–72.
8. Praslicka B, Ma C, Taran N. A computationally efficient high-fidelity multi-physics design optimization of traction motors for drive cycle loss minimization. IEEE Transactions on Industry Applications. 2023; 59(2): 1351–1360.
9. Roshandel E, Mahmoudi A, Soong WL, et al. Optimal design of induction motors over driving cycles for electric vehicles. IEEE Transactions on Vehicular Technology. 2023; 72(12): 15548–15562.
10. Madichetty S, Mishra S, Basu M. New trends in electric motors and selection for electric vehicle propulsion systems. IET Electrical Systems in Transportation. 2021; 11(3): 186–199. doi: 10.1049/els2.12018
11. Mahmouditabar F, Baker NJ. Design optimization of induction motors with different stator slot rotor bar combinations considering drive cycle. Energies. 2024; 17(1): 154.
12. Sweeting WJ, Hutchinson AR, Savage SD. Factors affecting electric vehicle energy consumption. International Journal of Sustainable Engineering. 2011; 4(3): 192–201. doi: 10.1080/19397038.2011.592956
13. Chau T, Li W. Overview of electric machines for electric and hybrid vehicles. International Journal of Vehicle Design. 2014; 64(1): 46–71. doi: 10.1504/IJVD.2014.057775
14. Gordić M, Stamenković D, Popović V, et al. Electric vehicle conversion: Optimization of parameters in the design process. Technical Gazette. 2017; 24(4): 1213–1219.
15. He L, Jing H, Zhang Y, et al. Performance research of integrated thermal management system for battery electric vehicles with motor waste heat recovery. Journal of Energy Storage. 2024; 84: 110893.
16. Wang Z, Ching TW, Huang S, et al. Challenges faced by electric vehicle motors and their solutions. IEEE Access. 2020; 9: 5228–5249. doi: 10.1109/ACCESS.2020.3045716
17. Janpoom K, Suttakul P, Achariyaviriya W, et al. Investigating the influential factors in real-world energy consumption of battery electric vehicles. Energy Reports. 2023; 9(s12): 316–320.
18. Suryavanshi S, Ghanegaonkar PM, Jadhav GK, et al. Comparative performance assessment of sizing of electric motor through analytical approach for electric vehicle application. ARAI Journal of Mobility Technology. 2023; 3(4): 842–855. doi: 10.37285/ajmt.3.4.7
19. Bajrami A, Palpacelli MC. A proposal for a simplified systematic procedure for the selection of electric motors for land vehicles with an emphasis on fuel economy. Machines. 2023; 11(4): 420.
20. Ehsani M, Gao Y, Longo S, et al. Modern Electric, Hybrid Electric, and Fuel Cell Vehicles, 3rd ed. CRC Press; 2018.
21. Gillespie TD. Fundamentals of Vehicle Dynamics. SAE International; 1992.
22. Suryavanshi SS, Ghanegaonkar PM. Repercussion of effect of different drive cycles on evaluation of electrical consumption for electric four-wheeler. Energy Storage. 2023; 5(7): e468.
23. Wankhede S, Thorat P, Shisode S, et al. Energy consumption estimation for electric two-wheeler using different drive cycles. Energy Storage. 2022; 4(6): e361.
24. Mamo T, Gebresenbet G, Gopal R, et al. Assessment of an electric vehicle drive cycle in relation to minimised energy consumption with driving behaviour: The case of Addis Ababa, Ethiopia, and its suburbs. World Electric Vehicle

Journal. 2023; 14(11): 302.
25. Kinoti E, Mosetlhe TC, Yusuff AA. Multi-criteria analysis of electric vehicle motor technologies: A review. World Electric Vehicle Journal. 2024; 15(12): 541.
26. Askerdal M, Fredriksson J, Laine L. Development of simplified air drag models including crosswinds for commercial heavy vehicle combinations. Vehicle System Dynamics. 2023; 62(5): 1085–1102.
27. Cheng R, Zhang W, Yang J, et al. Analysis of the effects of different driving cycles on the driving range and energy consumption of BEVs. World Electric Vehicle Journal. 2025; 16(3): 124.